Appendixes

Appendix A: Text

Text S1 Characterization methods

Field emission scanning electron microscope (SEM, Zeiss, Gemini 300, Germany) equipped with energy dispersive dpectroscopy (EDS, Oxford, X-Max^N 50, Germany) was applied to observe the micro morphology, distribution, and element composition of the coating on the surface of ceramic membranes. X-ray diffractometer (XRD, Bruker D8 advance, Bruker in Germany) was used to analyze the crystal structure of MXene-ceramic membranes at a scanning speed of 5 °/min. X-ray photoelectron spectrometer (XPS, Scientific K-Alpha, ThermoFisher Scientific in USA) was performed to determine valence bond and molecular structure of MXene-ceramic membranes. The recombination efficiency of photogenerated electrons and holes in the surface coating materials of ceramic membrane was detected by a photoluminescence spectrometer (PL, FLS980, Edinburgh Instruments in UK). Ultraviolet visible (UV-vis) absorption spectrum was obtained by a UV/VIS/NIR diffuse reflectance spectrophotometer (UV-3600i Plus, Shimadzu in Japan). The strength of the TiO_2/Ti_3C_2-ceramic membranes were tested by scratching using a nanoindenter (UNHT, CSM, Switzerland). Weight stability tests under thermal conditions were carried out using a thermogravimetric analyzer (DTA7300, Hitachi, Japan).

Text S2 Photocatalytic experimental setup

The photocatalytic experiment was carried out in a box-type photocatalytic device, which is composed of a high-pressure mercury lamp, cooling water circulation system and magnetic stirrer. The high-pressure mercury lamp with a power of 400 W mainly emits UV light with a wavelength of 365 nm, which was placed 15 cm in front of the target pollutant solution.

Text S3 Photocatalytic degradation

In this experiment, MB and CIP with a concentration of 10 mg/L were selected as the main target pollutants to evaluate the photocatalytic performance of the TiO_2/Ti_3C_2 photocatalytic membranes. The membrane was placed in a solution containing 270 mL of target pollutant solution facing the UV light source and then irradiated with UV light. Following the set time interval, a certain volume of pollutant solution was collected and measured by a UV spectrophotometer to obtain the residual concentration of contaminants. The corresponding absorbance of MB and CIP was analyzed at their maximum wavelength of 278 nm and 664 nm, respectively. The photocatalytic degradation rate of pollutants is expressed by the ratio of pollutant concentrations before and after photocatalytic degradation.

For the sake of optimizing the preparation conditions of the TiO_2/Ti_3C_2 photocatalytic membranes, conditional experiments were carried out to identify the effects of calcination temperature, load amount, and calcination time on the photocatalytic performance of the Ti_3C_2-TiO_2 photocatalytic membrane.

Text S4 Photocatalytic membrane cycling experiment

To evaluate the recycling performance of TiO_2/Ti_3C_2 ceramic membranes, the membranes were subjected to a photocatalytic cycling test as follows: after each photocatalytic experiment, the TiO_2/Ti_3C_2 ceramic membranes were extracted, rinsed with deionized water and then irradiated with ultraviolet light for 4 h. After the membranes had been thoroughly dried out at room temperature, the photocatalytic experiments were carried out once again, and the cycling experiments were repeated five times. The cycle was repeated 5 times.

Text S5 Determination of the intermediates

Degradation intermediates of CIP were determined by Agilent LC-QQQ-MS with triple quadrupole and ESI ion source. The mobile phases were methanol and water (0.1% formic acid) with a linear gradient at a flow rate of 200 μL/min. Detection was performed in positive ion mode. The ionization voltage was 4.0 kV, and the capillary temperature was 335℃.

Text S6 The toxicity assessment software and the methods taken

The Toxicity Estimation Software Tool (TEST) was developed to allow users to easily estimate the toxicity of chemicals using Quantitative Structure Activity Relationships (QSARs) methodologies. The developmental toxicity of the CIP to be evaluated is assessed by entering the intermediates of the CIP to be evaluated by entering a structural text file. The consensus method was used to assess developmental toxicity. The predicted toxicity is estimated by taking an average of the predicted toxicities from all QSAR methods (provided the predictions are within the respective applicability domains).

The Ecological Structure Activity Relationships (ECOSAR) Class Program is a computerized predictive system that estimates aquatic toxicity. The program estimates a chemical's acute (short-term) toxicity and chronic (long-term or delayed) toxicity to aquatic organisms, such as fish, aquatic invertebrates, and aquatic plants, by using computerized Structure-Activity Relationships (SARs).

The above software is recognized by the US Environmental Protection Agency. However, it is important to note that the biological toxicity of the prepared synthetic material cannot be assessed by above software.

Appendix B: Figure

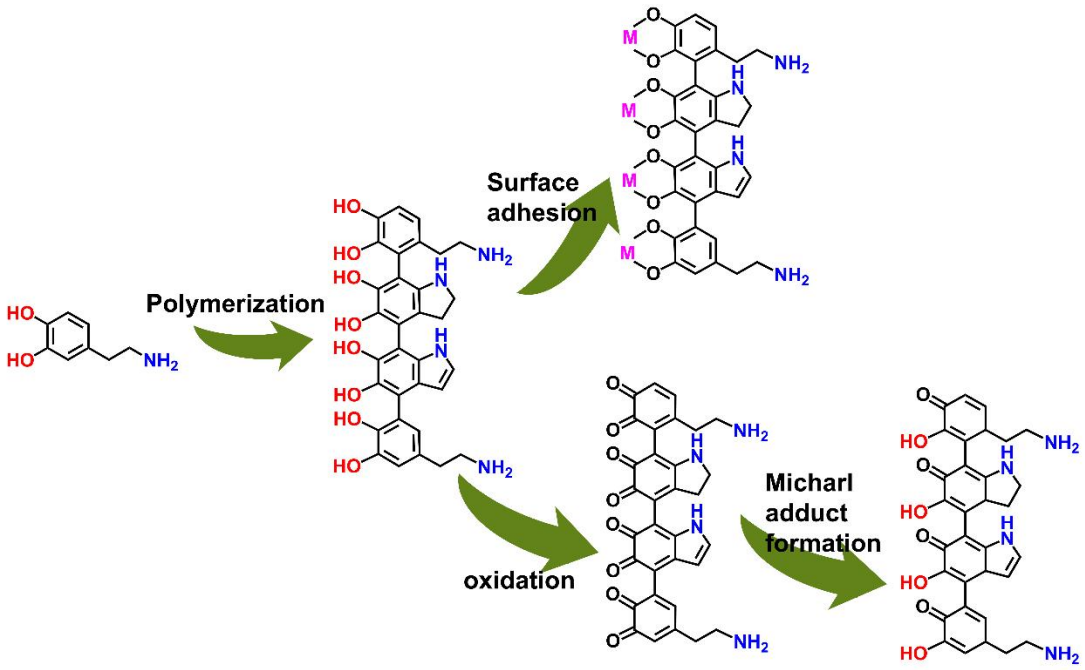

Fig. S1 Possible aggregation mechanism of PDA.

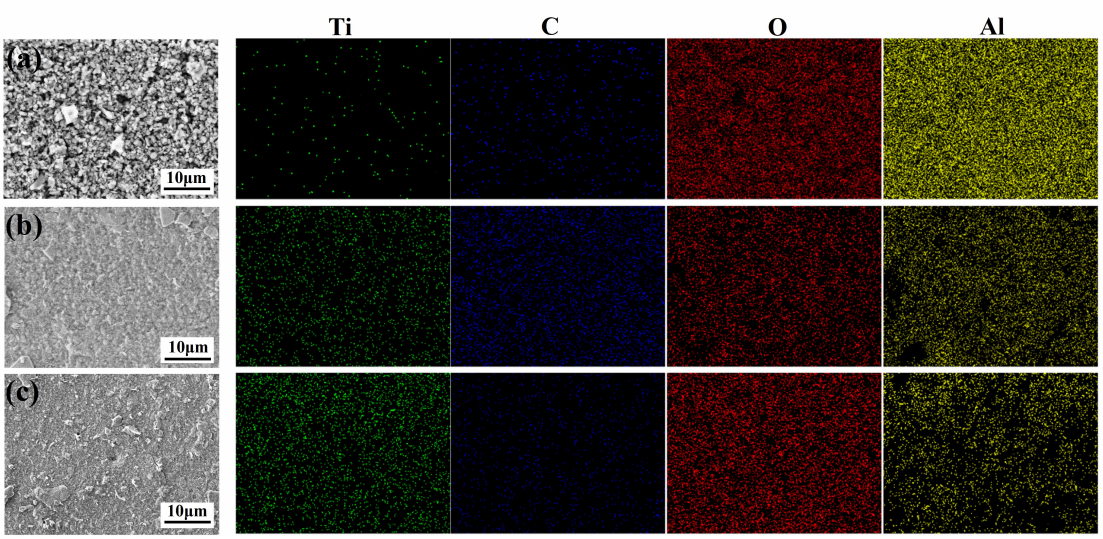

Fig. S2 EDS mapping images of the ceramic membrane surfaces: (a) raw ceramic membrane, (b) MT25 and (c) MT650.

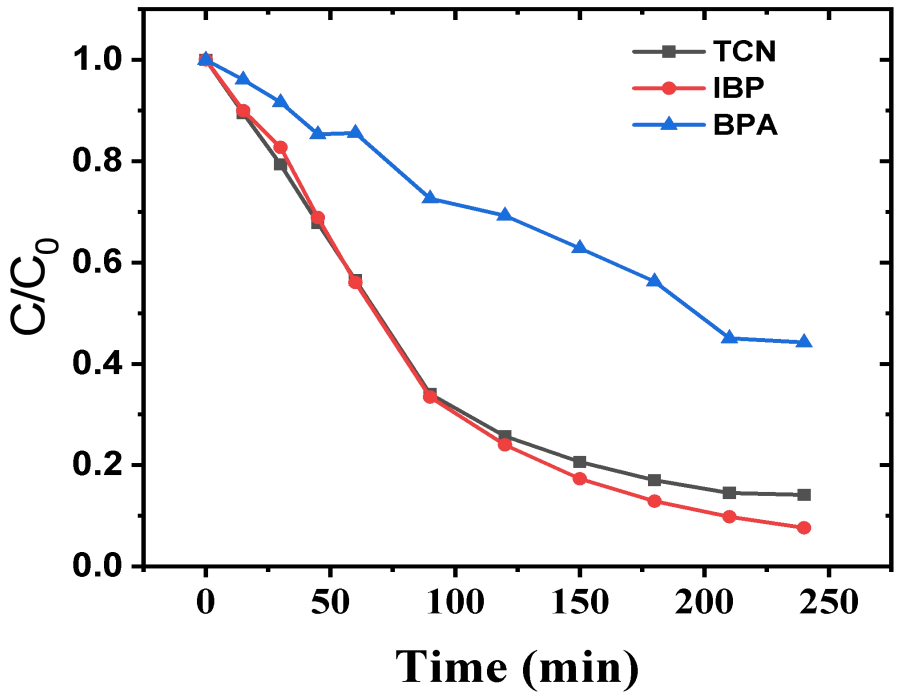

Fig. S3 The degradation curves for CIP, TCN, and BPA.

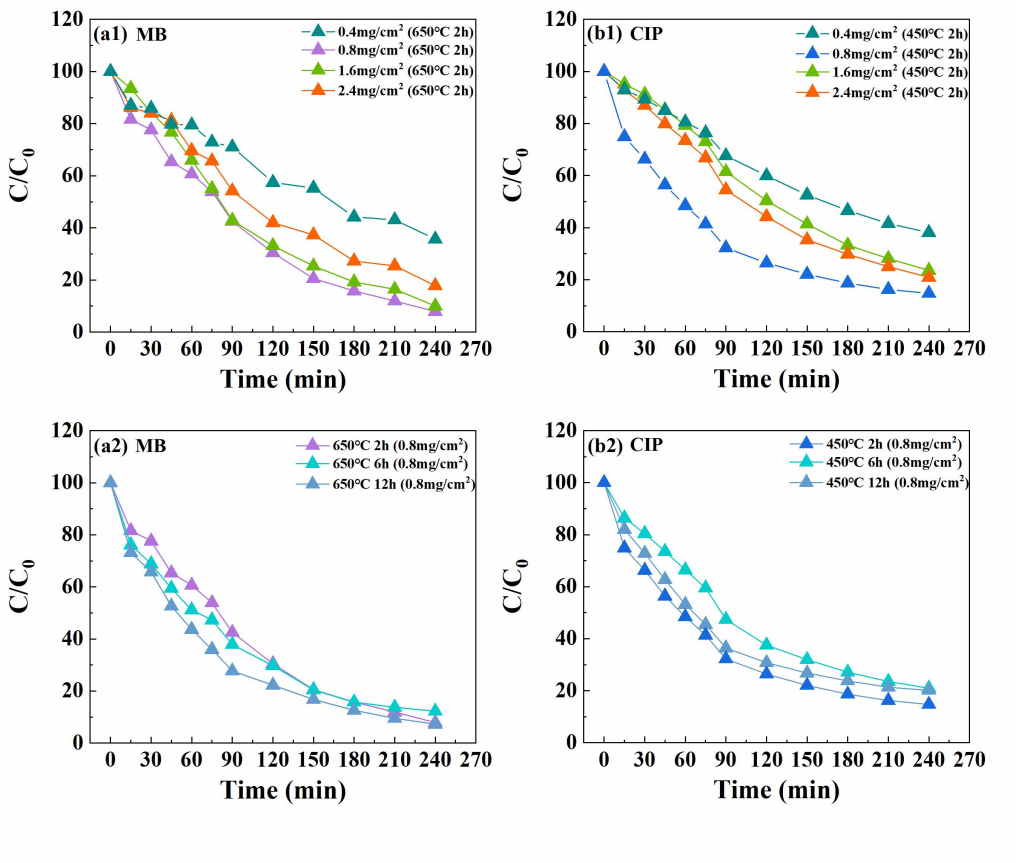

Fig. S4 Photocatalytic properties of Ti_3C_2/TiO_2 ceramic films with different Ti_3C_2 loadings ((a1) MB, (a2) CIP) and calcination times ((b1) MB, (b2) CIP).

Fig. S5 Surface images of membranes at different stages (after cleaning).

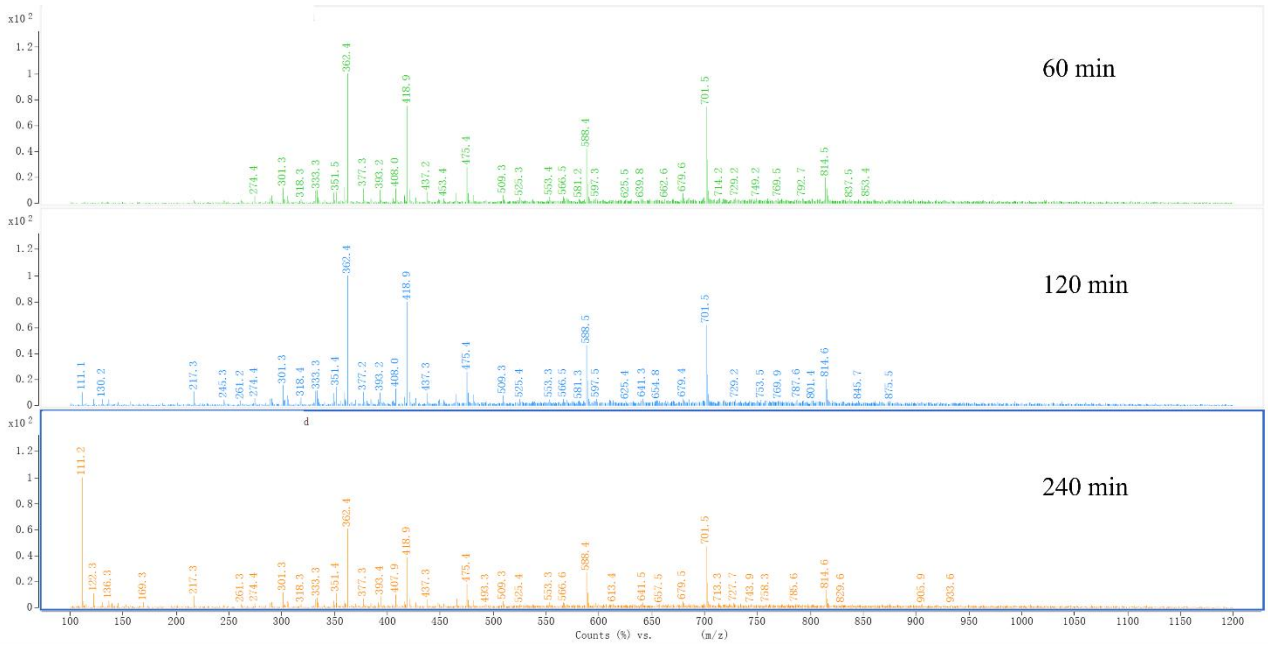

Fig. S6 LC-MS of the degradation products of CIP.

Appendix C: Table

Table S1 Comparison of degradation rates with other catalysts in the literature.

Catalysts or catalytic membrane	Pollution	K/min^{-1}	Reference
$rTiO_3$	MB	0.0022	(Chen et al., 2022)
Ag_2O	MB	0.0045	(Chen et al., 2022)
TiO_2(B)	MB	0.009	(Liu et al., 2021)
TiO_2/Ti_3C_2 ceramic membrane	MB	0.0104	this work
g-C_3N_4	MB	0.003	(Prabakaran et al., 2021)
Hydrophilic TiO_2/PES	MB	0.0094	(Fischer et al., 2015)
Hydrophilic TiO_2/PVDF membrane	MB	0.001	(Fischer et al., 2015)
BOC	CIP	0.00537	(Xue et al., 2023)
BMC	CIP	0.00644	(Xue et al., 2023)
TiO_2/Ti_3C_2 ceramic membrane	CIP	0.0106	this work
$CuBi_2O_4$	CIP	0.00298	(Fu et al.,2021)
BIOB	CIP	0.00704	(Fu et al.,2021)
g-C_3N_4	CIP	0.0021	(Li et al., 2023)
g-C_3N_4/TCNQ-10	CIP	0.0083	(Li et al., 2023)
TiO_2	CIP	0.00476	(Ding et al., 2022)
CoAl-LDH	CIP	0.00372	(Ding et al., 2022)
1% Bi/BiOCOOH/PVDF membrane	CIP	0.00985	(Shen et al., 2023)
PVDF membrane	CIP	0.00225	(Shen et al., 2023)

TiO_2/PVDF-TrFE membrane	CIP	0.01	(Martins et al., 2019)

References

Chen X, Qi H, Zhang C, Ma L, Li Z, Chen P, Xing Q, Sun Q, Yan Z (2022). Synthesis and characterization of recyclable PVA/$SrTiO_3$/Ag_2O composite with photocatalytic degradation performance of methylene blue. Applied Physics. A, Materials Science & Processing, 128(5): 374 doi:10.1007/s00339-022-05510-3

Ding C, Guo J, Gan W, Chen P, Li Z, Yin Z, Qi S, Deng S, Zhang M, Sun Z (2022). Ag nanoparticles decorated Z-scheme CoAl-LDH/TiO_2 heterojunction photocatalyst for expeditious levofloxacin degradation and Cr(VI) reduction. Separation and Purification Technology, 297: 121480 doi:10.1016/j.seppur.2022.121480

Fischer K, Grimm M, Meyers J, Dietrich C, Gläser R, Schulze A (2015). Photoactive microfiltration membranes via directed synthesis of TiO_2 nanoparticles on the polymer surface for removal of drugs from water. Journal of Membrane Science, 478: 49–57 doi:10.1016/j.memsci.2015.01.009

Fu S, Zhu H, Huang Q, Liu X, Zhang X, Zhou J (2021). Construction of hierarchical $CuBi_2O_4$/Bi/BiOBr ternary heterojunction with Z-scheme mechanism for enhanced broad-spectrum photocatalytic activity. Journal of Alloys and Compounds, 878: 160372 doi:10.1016/j.jallcom.2021.160372

Liu R, Zhao M, Zheng X, Wang Q, Huang X, Shen Y, Chen B (2021). Reduced graphene oxide/TiO_2(B) immobilized on nylon membrane with enhanced photocatalytic performance. Science of the Total Environment, 799: 149370 doi:10.1016/j.scitotenv.2021.149370

Li Q, Wen N, Zhang W, Yu L, Shen J, Li S, Lv Y (2023). Preparation of g-C_3N_4/TCNQ composite and photocatalytic degradation of pefloxacin. Micromachines, 14(5): 941 doi:10.3390/mi14050941

Martins P M, Ribeiro J M, Teixeira S, Petrovykh D Y, Cuniberti G, Pereira L, Lanceros-Méndez S (2019). Photocatalytic microporous membrane against the increasing problem of Water water emerging pollutants. Materials, 12(10): 1649 doi:10.3390/ma12101649

Prabakaran E, Velempini T, Molefe M, Pillay K (2021). Comparative study of KF, KCl and KBr doped with graphitic carbon nitride for superior photocatalytic degradation of methylene blue under visible light. Journal of Materials Research and Technology, 15: 6340–6355 doi:10.1016/j.jmrt.2021.10.128

Shen Y, Xu H, Zheng Y, Wang Y, Zhang L, Zhang Z, Zhong L, He Z (2023). Fabrication of Bi/BiOCOOH/PVDF with improved photocatalytic activity for the degradation of ciprofloxacin. Surfaces and Interfaces, 42: 103483 doi:10.1016/j.surfin.2023.103483

Xue J, Xiao W, Shi L, Liu Y, Wang P, Bi Q (2023). Efficient degradation of ciprofloxacin by a flower-spherical Bi_2MoO_6/BiOCl Z-type heterojunction photocatalyst enriched with oxygen vacancies. Journal of Environmental Chemical Engineering, 11(6): 111235 doi:10.1016/j.jece.2023.111235